Atmos. Chem. Phys. Discuss., 14, 7823–7857, 2014
www.atmos-chem-phys-discuss.net/14/7823/2014/
doi:10.5194/acpd-14-7823-2014

Atmospheric Chemistry and Physics Discussions

Comparison of HONO budgets for two measurement heights at a field station within the boreal forest (SMEAR II – HUMPPA-COPEC 2010)

R. Oswald[1,2], M. Ermel[1,2], K. Hens[3], A. Novelli[3], H. G. Ouwersloot[3,4], P. Paasonen[5], T. Petäjä[5], M. Sipilä[5], P. Keronen[5], J. Bäck[6], R. Königstedt[3], Z. Hosaynali Beygi[3], H. Fischer[3], B. Bohn[7], D. Kubistin[3,*], H. Harder[3], M. Martinez[3], J. Williams[3], T. Hoffmann[2], I. Trebs[1,], and M. Sörgel[1]**

[1]Biogeochemistry Department, Max Planck Institute for Chemistry, P.O. Box 3060, 55020 Mainz, Germany
[2]Institute for Inorganic and Analytical Chemistry, Johannes Gutenberg University Mainz, 55128 Mainz, Germany
[3]Airchemistry Department, Max Planck Institute for Chemistry, 55128 Mainz, Germany
[4]Meteorology and Air Quality, Wageningen University, Wageningen, the Netherlands
[5]Deptartment of Physics, P.O. Box 64, 00014 University of Helsinki, Finland
[6]Department of Forest Sciences, P.O. Box 27, 00014 University of Helsinki, Finland

[7]Institut für Energie- und Klimaforschung IEK-8: Troposphäre, Forschungszentrum Jülich GmbH, 52428 Jülich, Germany
[*]now at: University of Wollongong, School of Chemistry, Wollongong, Australia
[**]now at: Centre de Recherche Public – Gabriel Lippmann, Department Environment and Agro-biotechnologies, 41 rue du Brill, 4422 Belvaux, Luxembourg

Received: 28 February 2014 – Accepted: 5 March 2014 – Published: 21 March 2014

Correspondence to: M. Sörgel (m.soergel@mpic.de)

Published by Copernicus Publications on behalf of the European Geosciences Union.

Abstract

Atmospheric concentrations of nitrous acid (HONO), one of the major precursors of the hydroxyl radical (OH) in the troposphere, normally exceed by far the values predicted by the assumption of a photostationary state (PSS) during daytime. Therefore, additional sources of HONO were intensively investigated in the last decades. Here, we present budget calculations of HONO based on simultaneous measurements of all relevant species including HONO and OH at two different measurement heights, i.e. 1 m above ground and about 2 to 3 m above canopy (24 m above ground), conducted in boreal forest environment. We observed mean HONO concentrations during daytime of about 6.5×10^8 molecules cm^{-3} (26 ppt), more than twenty times higher than expected from the PSS, 0.2×10^8 molecules cm^{-3} (1 ppt). To close the budgets in both heights a strong additional source term during daytime is required. This unidentified source is maximal at noon (up to 1.1×10^6 molecules cm^{-3} s^{-1}, 160 ppt h^{-1}) and in general up to 2.3 times stronger above the canopy than close to the ground. The insignificance of known gas phase reactions and also other processes like dry deposition or advection compared to the photolytic decomposition of HONO at this measurement site was an ideal prerequisite to study possible correlations of this unknown term to proposed HONO sources. But neither the proposed emissions from soils nor the proposed photolysis of adsorbed HNO_3 contributed substantially to the unknown source. However, the unknown source was found to be perfectly correlated to the unbalanced photolytic loss of HONO.

1 Introduction

Since the first unequivocal detection of HONO in the atmosphere by Perner and Platt (1979), its formation and fate as well as its contribution to primary OH production has been intensively studied (Lammel and Cape, 1996; Kleffmann, 2007). Recently, the importance of HONO in atmospheric chemistry and its implications has been demonstrated using a global chemistry transport model (Elshorbany et al., 2012). While the

fate of HONO is mainly determined by the photolytic decomposition producing OH, the major uncertainty in modelling studies results from the lack of understanding the HONO formation pathways. Budget calculations of the postulated sources and sinks (Kleffmann et al., 2005; Su et al., 2008c; Sörgel et al., 2011a) have usually been used to quantify the magnitude of the missing source term. Only a few source estimates derived from flux measurements have been published up to now (Zhang et al., 2012; Zhou et al., 2011; Ren et al., 2011). The current status of HONO formation and loss pathways, important for atmospheric chemistry is as follows.

The major sink during daytime for HONO is the homolytic cleavage of the O-N single bond by radiation ($\lambda < 400$ nm), determined by the photolysis frequency, J(HONO).

$$\mathrm{HONO} \xrightarrow{h\nu} \mathrm{OH} + \mathrm{NO} \qquad \text{(R1)}$$

Since OH is produced, this reaction is of primary importance to atmospheric photochemistry. J(HONO) shows a similar wavelength dependency as the photolysis frequency of nitrogen dioxide (NO_2), $J(NO_2)$ (Kraus and Hofzumahaus, 1998). Therefore, J(HONO) can be linked to $J(NO_2)$ by using the approach of Trebs et al. (2009):

$$J(\mathrm{HONO}) = 0.17 \times J(\mathrm{NO_2}) \qquad (1)$$

The back reaction of Reaction (R1) in presence of a third body, Reaction (R2), can reform HONO with a rate constant (k_2 at 298 K and 1013 hPa) of $(7.4 \pm 1.3) \times 10^{-12}$ cm^3 molecules^{-1} s^{-1} (Sander et al., 2011).

$$\mathrm{OH} + \mathrm{NO} \xrightarrow{M} \mathrm{HONO} \qquad \text{(R2)}$$

While the gas phase reaction of OH with NO forms HONO, OH may also react with HONO and reform NO_x.

$$\mathrm{HONO} + \mathrm{OH} \rightarrow \mathrm{NO_2} + \mathrm{H_2O} \qquad \text{(R3)}$$

Due to the in general low concentrations of HONO and OH compared to NO this reaction is less important than Reaction (R2) even with a similar reaction rate constant (k_3 at 298 K and 1013 hPa) of about 6.0×10^{-12} cm^3 molecules^{-1} s^{-1} (Atkinson et al., 2004) and constitutes typically less than 5 % of the total HONO loss (Su et al., 2008c; Sörgel et al., 2011a).

A surface reaction of NO_2 and H_2O was suggested as another formation pathway for HONO. Finlayson-Pitts et al. (2003) proposed a mechanism, whereby NO_2 after dimerization is dissolved in a humid surface film. The formed N_2O_4 rearranges into the mixed anhydride of nitrous acid and nitric acid ($ONONO_2$), which rapidly dissolves into HONO and nitrate.

$$2NO_2(g) + H_2O(l) \rightarrow HONO(g) + H^+(aq) + NO_3^-(aq) \quad \text{(R4)}$$

Yabushita et al. (2009) and De Jesus Medeiros and Pimentel (2011) further investigated the mechanism with focus on the NO_2 uptake and the kinetics of the initial hydrolysis. The reaction rate constant of Reaction (R4) is difficult to determine in the field, but can be estimated with the approach of Alicke et al. (2002).

$$k_4^{\text{dark}} = \frac{[\text{HONO}]_{\text{max}} - [\text{HONO}]_{\text{sunset}}}{(t_{\text{max}} - t_{\text{sunset}}) \times \overline{[\text{NO}_2]_{t_{\text{sunset}}}^{t_{\text{max}}}}} \quad (2)$$

After sunset the concentration of HONO, $[HONO]_{sunset}$, increases and reaches a maximum, $[HONO]_{max}$. The difference between $[HONO]_{max}$ and $[HONO]_{sunset}$ divided by the product of the elapsed time ($t_{max} - t_{sunset}$) and the average NO_2 concentration during that time, $\overline{[NO_2]_{t_{sunset}}^{t_{max}}}$, determines the rate of heterogeneous HONO formation during the night. The reaction rates found for nighttime conversion range from 0.4 (Kleffmann et al., 2003) to 2.0 ppb(HONO) × ppb(NO_2)$^{-1}$ × h^{-1} (Sörgel et al., 2011a). This approach is only valid, if the heterogeneous dark Reaction (R4) is the dominant source of HONO during night.

Beside the dark reaction of NO_2, ortho-nitrophenols, o-NPs, can photolytically decompose to form HONO as a side product (Bejan et al., 2006).

$$\text{o-NPs} \xrightarrow{h\nu} [\text{products}]^* + \text{HONO} \quad \text{(R5)}$$

The authors propose parts of the reaction mechanism, but since they could not measure the main products, the exact and complete mechanism is not yet clarified. It is further stated that this source might be of primary interest for the atmosphere under urban conditions, where possibly 1 ppb of o-NPs occurs. Since the o-NPs absorb light in a similar wavelength range as NO_2, one can estimate the photolysis by an upper limit approach (Bejan et al., 2006),

$$J(\text{o-NPs}) = 2.5 \times 10^{-3} \times J(\text{NO}_2) = 1.4 \times 10^{-2} \times J(\text{HONO}) \quad (3)$$

In addition to the reaction of NO_2 with surface adsorbed water (Reaction R4), Stemmler et al. (2006) and (2007) found that a surface film or aerosol of humic acid (HA) can act as photosensitizer when irradiated and reduces NO_2 to HONO.

$$\text{HA} \xrightarrow{h\nu} \text{A}^{\text{red}} + \text{X}^{\text{ox}} \quad \text{(R6)}$$

$$\text{A}^{\text{red}} + \text{X}^{\text{ox}} \rightarrow \text{HA}' \quad \text{(R7)}$$

$$\text{A}^{\text{red}} + \text{NO}_2 \rightarrow \text{HA}'' + \text{HONO} \quad \text{(R8)}$$

HA naturally occurs in the environment for example in soil. Hence, soil might act as a source for HONO under irradiation in the UV and exposure to NO_2 (Stemmler et al., 2006). Other reactants than A^{red} in Reaction (R8) might also be reductive. E.g. fresh soot particles are supposed to reduce NO_2 and form HONO. This source is only important for high NO_2 concentrations and environments with freshly emitted soot (Aubin and Abbatt, 2007; Monge et al., 2010).

It was shown by several studies (Kubota and Asami, 1985; Twigg et al., 2011; Su et al., 2011; Oswald et al., 2013) that soils can emit HONO. Decreasing soil water content and hence drying out of soil leads to an increase in soil aeration with emission

of trace gases, namely N_2O, NO and HONO. Due to the complexity of soil emission fluxes, depending on biological, physical and chemical processes and properties of soil, it is not straight forward to calculate the source strength, although observed NO emissions might serve as a proxy for HONO emission fluxes (Oswald et al., 2013).

Surface adsorbed nitric acid $HNO_{3(ads)}$ either deposited or directly formed during the reaction cascade of (R4), is proposed to be photolytically sensitive and might decompose to HONO in the UV (Zhou et al., 2011).

$$\begin{aligned} &HNO_{3(ads)} \xrightarrow{h\nu} [HNO_{3(ads)}]^* \\ &[HNO_{3(ads)}]^* \rightarrow HONO_{(ads)} + O(^3P)_{(ads)} \qquad \text{(R9)} \\ &HONO_{(ads)} \leftrightharpoons HONO_{(g)} \end{aligned}$$

The production of HONO by photolysis of $HNO_{3(ads)}$ depends on the physicochemical state of the surface. While for dry surfaces (relative humidity (RH) = 0 %) NO_x is the major product, relative humidity of about 20 % suffices to increase the HONO yield (Zhou et al., 2003). According to Goodman et al. (2001), at 20 % RH there should be at least a monolayer of water present on the surface. Zhou et al. (2003) further propose that $NO_{2(ads)}$ formed during the photolysis of $HNO_{3(ads)}$ may also react further via Reaction (R4), which not only forms HONO, but also recovers parts of HNO_3. Later Zhou et al. (2011) suggested that the formed NO_2 is reduced to HONO via the mechanism of Reactions (R6) and (R8) proposed by Stemmler et al. (2006). However, the rate of HONO formation depends on the amount of HNO_3 available on irradiated surfaces and the photolysis frequency of HNO_3, $J(HNO_3)$, which is enhanced by adsorption to surface compared to gas phase photolysis (Zhu et al., 2008, 2010). Depending on the type of surface the enhancement factor varies; Zhou et al. (2003) found an enhancement of about 2 orders of magnitude by HNO_3 adsorption on borosilicate glass (see also Ramazan et al., 2004), while Baergen and Donaldson (2013) calculated an enhancement of about 4 orders of magnitude by HNO_3 adsorbed to grime.

Other loss terms than Reactions (R1) and (R3) include the dry and wet deposition of HONO. The dry deposition of HONO depends on the ambient mixing ratio of HONO,

on turbulent mixing within the planetary boundary layer and the ability of terrestrial surfaces to take up HONO. With a Henry coefficient of 49 M atm^{-1} (Park and Lee, 1988), wet deposition of HONO is quite efficient. After a rain event mixing ratios of HONO strongly decrease (Sörgel et al., 2011b).

Assuming only the known gas phase Reactions (R1)–(R3) contribute to the HONO formation, a photostationary state should be established (Kleffmann et al., 2005),

$$\frac{d[HONO]_{PSS}}{dt} = k_2[NO][OH] - J(HONO)[HONO]_{PSS} - k_3[OH][HONO]_{PSS} = 0 \qquad (4)$$

$$\Rightarrow [HONO]_{PSS} = \frac{k_2[NO][OH]}{J(HONO) + k_3[OH]} \qquad (5)$$

This equilibrium can only explain a minor portion of gas phase HONO observed at remote and rural sites (Kleffmann, 2007; Su et al., 2008b; Sörgel et al., 2011a; Wong et al., 2012), but may play an important role for measurement results obtained in urban areas (Lee et al., 2013). The budget calculations of Sörgel et al. (2011a) and Li et al. (2012) showed that including heterogeneous reactions of NO_2 (Reaction R4) only slightly improves the discrepancy between $[HONO]_{PSS}$ and measured HONO mixing ratios.

In this study, we present the results of the field campaign HUMPPA-COPEC 2010 (**H**yytiälä **U**nited **M**easurement of **P**hotochemistry and **P**articles in **A**ir – **C**omprehensive **O**rganic **P**recursor **E**mission and **C**oncentration study) related to HONO chemistry and we provide a detailed overview of its sources and sinks using a budget calculation for two measurement heights, i.e. below and above a boreal forest canopy. We explicitly analyse additional source terms, like HONO emission by soil and the formation of HONO by photolysis of $HNO_{3(ads)}$.

2 Experimental

The HUMPPA-COPEC 2010 was a comprehensively instrumented intensive field measurement campaign, performed from 12 July until 12 August at the SMEAR II site (Station for Measuring Ecosystem-Atmosphere Relation; 61.846° N, 24.295° E) located in the boreal forest in Hyytiälä (Williams et al., 2011).

HONO was measured using two Long Path Absorption Photometer instruments (LOPAP, QUMA Elektronik & Analytik, Wuppertal, Germany). A detailed description of the instrument has been given by Kleffmann et al. (2002) and Heland et al. (2001). Briefly, an acidic solution of sulfanilamide is used to sample HONO with a stripping coil. HONO is transformed rapidly into a diazonium salt, the precursor of diazotation, carried out in sequence. The concentration of the azo dye formed is equivalent to the concentration of HONO in the sampled air and is measured by a VIS-photometer. The intercomparison of both LOPAP instruments used in this study has been described in detail by Sörgel et al. (2011b) and showed a good agreement (within 12 % relative error) under dry conditions (no rain or fog). The inlets of the two instruments were positioned at about 1 m and 24 m above ground (canopy top height 20 to 21 m). Both instruments ran with a response time of below 10 min and lower limit of detection ranging from 0.2 to 1.3 ppt during campaign.

A laser induced fluorescence (LIF) instrument to measure the atmospheric concentration of the hydroxyl radical, OH, based on the fluorescence assay by gas expansion technique (FAGE) (Hens et al., 2013; Novelli et al., 2014) measured OH above the canopy at a height of about 24 m, while a chemical ionization mass spectrometer (CIMS; Petäjä et al., 2009) measured OH near to the ground at about 1 m. The two different systems were compared under field conditions, measuring at 1 m above ground level and showed reasonable agreement (Hens et al., 2013). Lower detection limits of LIF and CIMS were about 9×10^5 molecules cm^{-3} and 5×10^4 molecules cm^{-3}, respectively.

NO and NO_x were monitored by high resolution and high sensitivity chemiluminescence detectors, a TEI 42C TL (Thermo Fisher Scientific, US) with a limit of detection of about 0.1 ppb positioned at 4 m, and a modified (Hosaynali Beygi et al., 2011) CLD 790 SR with a detection limit of about 16 ppt (ECO-Physics, Switzerland) positioned at 24 m above ground. Both instruments use a blue light converter for efficient and selective transformation of NO_2 to NO. In addition ozone, O_3, was measured by a UV-absorption photometer above canopy.

The photolysis rates of NO_2 and O_3, $J(NO_2)$ and $J(O^1D)$, respectively, were measured using filter radiometers (Meteorologie consult, Königstein, Germany; Bohn et al., 2008). Two $J(NO_2)$ sensors were positioned at 2 m and 24 m above ground, and one $J(O^1D)$ sensor was placed at 24 m. Each measured the downwelling radiation.

Relative humidity, temperature, wind direction, wind speed and other meteorological parameters were monitored routinely by the SMEAR II station (Junninen et al., 2009; http://www.atm.helsinki.fi/smartSMEAR/).

Evaluation of the boundary layer height was determined by radiosondes, measuring relative humidity, temperature, pressure and altitude. From this data vertical profiles of the potential temperature and the specific humidity were gained and hence the height and type of boundary layer have been inferred (Ouwersloot et al., 2012).

A sample from the O-horizon of soil was taken at 10 June 2012 at the measurement site and was measured under controlled conditions in the lab according to Oswald et al. (2013) to investigate NO and HONO emission fluxes from soil.

3 Results

During the measurement period of HUMMPA-COPEC 2010 from 12 July to 12 August 2010, not all instruments were running continuously. Beside specific instrument malfunctions, several power disruptions caused by thunderstorms often interrupted the measurement. From 17 July until 5 August, the two LOPAP instruments were running about 30 % of the time simultaneously. The dataset of other measurements is close to

complete for this period, except for the OH measurement above the canopy and the $J(NO_2)$ measurement below the canopy (see Fig. 1). The same situation is found for J(HONO) below the canopy, hence it was calculated from $J(NO_2)$ according to Eq. (1).

Aside from a linear relationship found between OH measured at the forest floor and above canopy (Fig. 2), the exponential relationship of $J(NO_2)$ at 2 m above ground and $J(NO_2)$ at 24 m above ground, was used to interpolate OH above the canopy and $J(NO_2)$ below the canopy to extend the data basis for PSS calculations.

3.1 Diel variation of HONO

In the clean environment of Hyytiälä diurnal variations of HONO were observed with mean daytime concentrations of 6.6×10^8 molecules cm^{-3} (27 ppt) at 1 m height and 6.5×10^8 molecules cm^{-3} (26 ppt) at 24 m height and mean nighttime concentrations of 9.1×10^8 molecules cm^{-3} (37 ppt) at 1 m height and 9.2×10^8 molecules cm^{-3} (37 ppt) at 24 m. Maximum values reached 3.2×10^9 molecules cm^{-3} (132 ppt) at 1 m and 3.4×10^9 molecules cm^{-3} (138 ppt) at 24 m at 22:30 UTC+2 in the late evening of 2 August. The concentrations reached a minimum after a short and strong rain event in the morning of the 25 July with values below 2 ppt close to the detection limit. The concentrations of HONO were calculated according to Eq. (5) by assuming a PSS, only valid for conditions with short photolytic lifetime of HONO. In agreement with Kleffmann et al. (2005) and Sörgel et al. (2011a) the box plots in Fig. 3 obviously show that for both heights the calculated concentrations are often more than one order of magnitude lower than the measured concentration of HONO. While the PSS calculation shows a peak in the morning (6:30) at 1 m height and around mid-morning (8:30) at 24 m height, the daytime measured HONO values peak at noon (11:30).

Sörgel et al. (2011a) stated that $[HONO]_{PSS}$ correlates best with measured [NO] and found neither a correlation to measured [OH] nor to measured J(HONO). The correlation between $[HONO]_{PSS}$ and [NO] was strong also in our data (Fig. 4). The reasonable correlation of $[HONO]_{PSS}$ to measured [NO] might serve as a proxy for

$[HONO]_{PSS}$ in general, since the ratio seems to be quite constant.

$$\frac{[HONO]_{PSS}}{[NO]} = \frac{k_2[OH]}{J(HONO) + k_3[OH]} \cong 0.02 \quad (6)$$

J(HONO) at PSS shows values of about 2 orders of magnitude higher than k_2 or k_3 multiplied with the [OH]. Since OH formation is strongly linked to radiation (Rohrer and Berresheim, 2006), its concentration positively correlates with J(HONO). Therefore, NO drives the variability of the PSS.

3.2 HONO budget calculations

The two gas phase Reactions (R2) and (R3) together with the photolysis fail to explain the observed HONO concentrations. The comparison of observed changes in HONO concentrations with calculated values considering further sources and sinks leads to a more complete understanding of HONO cycling.

$$\underbrace{\frac{\Delta[HONO]}{\Delta t}}_{\text{observed}} = \underbrace{\text{Sources} - \text{Sinks}}_{\text{calculated budget}} \quad (7)$$

If the calculated difference in sources and sinks equals the observed value, the budget would be closed. As mentioned before, normally this is not the case and an unknown source is missing, which can be calculated according to Su et al. (2008c) and Sörgel et al. (2011a) with the following equation:

$$P_{\text{unknown}} = \underbrace{\frac{\Delta[HONO]}{\Delta t}}_{\text{observed}} - \underbrace{k_2[NO][OH]}_{\text{R2: } P_{NO+OH}} - \underbrace{k_4^{\text{dark}}[NO_2]}_{\text{R4: } P_{het}} + \underbrace{J(HONO)[HONO]}_{\text{R1: } L_{phot}}$$
$$+ \underbrace{k_3[OH][HONO]}_{\text{R3: } L_{HONO+OH}} + \underbrace{\frac{v_{dep}}{h_{BL}}[HONO]}_{\text{dry deposition: } L_{dep}} + \underbrace{\pm T_h \pm T_v}_{\text{horizontal and vertical transports}} \quad (8)$$

The resulting $P_{unknown}$ shows, that for most of the day there is still a large source missing (Fig. 5), at least for the period from 6:00 in the morning to 20:00 in the evening where HONO lifetimes are below 30 min. This source is dominated by the photolytic loss of HONO that forms the major sink for HONO and which exceeds the considered sources by far.

Not only the known sources seem to be small compared with the photolytic loss rate, also the other sinks are negligible. E.g. with a deposition velocity for HONO of $2\,cm\,s^{-1}$ (Harrison et al., 1996; Su et al., 2008a), a mean daytime HONO concentration of 6.6×10^8 molecules cm^{-3} and a typical boundary layer height at midday of about 1000 m, the deposition rate is 1.3×10^3 molecules $cm^{-3}\,s^{-1}$, i.e. $1.9\,ppt\,h^{-1}$ and thus 1 to 2 orders of magnitude less than the photolytic loss. The very low contribution of the dry deposition to HONO loss has already been reported for other measurement campaigns (Su et al., 2008c; Sörgel et al., 2011a).

Horizontal transport, T_h, can strongly influence budget calculations in urban regions (Lee et al., 2013). However, Hyytiälä is surrounded by uniform boreal forest with up to 95 % of the area within 5 km radius being forested, mostly by Scots pine and Spruce trees (Williams et al., 2011) representing a homogenous fetch. Furthermore, with an average J(HONO) of about $6.7 \times 10^{-4}\,s^{-1}$, corresponding to a HONO lifetime of about 25 min and an average horizontal wind speed of $2\,m\,s^{-1}$ (maximum $7\,m\,s^{-1}$), direct emissions of HONO will be transported about 3 km (maximum 10 km) within one lifetime. As most of the surrounding is covered by forest and the next city Tampere, being nearly 50 km away there are no significant emission sources within the fetch, thus horizontal advection of direct emissions will have little influence on the HONO concentration during day. Therefore, the measurement site of SMEAR II, with its homogeneous fetch is well suited to analysing the behaviour of $P_{unknown}$, because all processes disturbing the analysis like horizontal transport and direct emissions can be neglected.

The contribution of vertical transport, T_v, to surface loss of HONO was estimated to be about 50 to 60 % (Wong et al., 2013), thus being the dominant loss process for HONO close to the ground. Vertical mixing acts as a sink close to the surface and as

an additional, yet unaccounted source term at elevated levels. Hence, depending on the concentration gradient of HONO and the ratio of photolysis, vertical transport can lead to reciprocal changes in $P_{unknown}$ above canopy and below canopy when using the budget approach.

3.3 Tracing the missing source

3.3.1 Influence of $J(NO_2)$ on $P_{unknown}$

Reactions (R5)–(R8) comprise several mechanisms of HONO formation from photolytic dissociation of ortho-nitrophenols or light induced conversion of NO_2 on different reductive surfaces, which are thought to be possible major sources for HONO during daytime (Stemmler et al., 2006). The wavelength range for the proposed reactions is mostly covered and well described by $J(NO_2)$. Therefore, a source corresponding to these reactions should correlate to $J(NO_2)$ and especially the light induced conversion of NO_2 should correlate even better with $P_{unknown}$ scaled to the NO_2 concentration (Fig. 6) (Sörgel et al., 2011a).

Scaling $P_{unknown}$ with the concentration of NO_2 on the ground leads to higher scattering of data points, which might be caused by the higher noise levels of NO_2 data on ground. On the contrary, the correlation above canopy is improved with similar scaling (Fig. 6b and d). The data points most affected belong to a period of rather cold and very clean conditions with low NO_2 concentration of 1.6 to 2.9×10^9 molecules cm^{-3} (65–118 ppt) at the 23 July (Williams et al., 2011). Since scaling $P_{unknown}$ above the canopy with corresponding NO_2 concentration increases the correlation with $J(NO_2)$, leads to the assumptions that either NO_2 plays a direct role in HONO formation or that in general NO_2 is a tracer for reactive nitrogen (other potential HONO precursors) in the atmosphere. The fact that the correlation between $P_{unknown}$ and $J(NO_2)$ below the canopy descends by scaling $P_{unknown}$ with NO_2 concentrations can be either due to data scattering as mentioned above, due to HONO deposition on the forest floor (Sörgel et al., 2014) or due to different pathways of HONO and NO_2 formation below

canopy. NO_2 below canopy is formed by shifted PSS below canopy and additional NO soil emissions oxidized by O_3 (Rummel et al., 2002). Opposed, due to low OH and NO values below canopy, the shift in the $[HONO]_{PSS}$ by reduced radiation below canopy has minor influence on HONO values (Fig. 3).

With our data set it is not possible to rule out that photolytic conversion of ortho-nitrophenols is a possible pathway, since there were no measurements of these species. However, from Eq. (3) one can estimate that the concentration of o-NPs has to exceed the concentration of HONO by a factor of about 70 in order to compensate the photolytic loss of HONO. Taking the average daytime mixing ratio of HONO above canopy, the resulting mixing ratio of o-NPs would be about 1.8 ppb. Based on earlier studies (Bejan et al., 2006; Kourtchev et al., 2013), the concentration in clean environment such as Hyytiälä should be much lower and thus insignificant for HONO formation.

Another possible $J(NO_2)$ depending source for HONO is the photolytic activation of organic surface reactants (Reactions R6–R8) to reduce NO_2 and form HONO (Stemmler et al., 2006). But as before, due to the lack of in-situ measurements of all parameters, this contribution could not be quantified. Obviously, there are many possibilities for humic acids or similar compounds to occur in the highly organic surrounding of the boreal forest. A strong hint on such a source might be the merging effect on the correlation of the $P_{unknown}$ with $J(NO_2)$ by scaling with the concentration of NO_2 above the canopy.

3.3.2 Indirect influence of $J(NO_2)$ on $P_{unknown}$

Besides the activation or the photolytic reaction of molecules by $J(NO_2)$, the radiation influences also other parameters. One of these is the temperature of soil. The temperature of soil surface changes stronger and faster than in deeper layers of soil and is driven by radiative heating and cooling. Nitrification and denitrification by microorganisms takes place at the uppermost layer of soil and produces reactive nitrogen gases (Conrad, 1996). The rate of reactive nitrogen formation depends on many parameters

like soil water content (SWC), pH, nutrient availability and, important in this context, the temperature of soil (Skopp et al., 1990; Oswald et al., 2013). Therefore, radiation can accelerate the formation of HONO by soil.

Since we did not measure the potential emission of HONO by soil in the field, a soil sample was taken afterwards and measured in the lab under controlled conditions according to Oswald et al. (2013). Concentrations of nutrients were quite low with ammonium being $(1.60 \pm 0.56)\,mg\,kg^{-1}$ N-NH_4^+, while NO_3^- and nitrite (NO_2^-) were not measureable (below LOD, i.e. $2\,mg\,kg^{-1}$ N-NO_3^- and $0.07\,mg\,kg^{-1}$ N-NO_2^-). This is in good agreement with Korhonen et al. (2013), who found that the measurement site of Hyytiälä provides nutrient poor soils with NH_4^+ as the dominant inorganic nitrogen compound in the extract of soil organic layer ($0.31\,kg\,ha^{-1}$ N-NH_4^+) and the first 30 cm of mineral soil, while NO_3^- forms only 0.6 % of it. The soil pH was very low with a value of about 3.0. The measurement of the soil sample showed no significant emission fluxes of HONO being below the limit of detection ($0.08\,ng\,m^{-2}\,s^{-1} = 0.288\,\mu g\,m^{-2}\,h^{-1}$) and emission fluxes of NO scattering around the limit of detection ($1\,ng\,m^{-2}\,s^{-1} = 3.6\,\mu g\,m^{-2}\,h^{-1}$). This is in good agreement with Oswald et al. (2013) and Maljanen et al. (2013), who both found that acidic forest soils tend to low emission fluxes of HONO. Maljanen et al. (2013) measured a maximum HONO flux of about $2\,\mu g\,m^{-2}\,h^{-1}$ in terms of N. This would equal a source-strength of 7.1×10^3 molecules $cm^{-3}\,s^{-1}$ ($1\,ppt\,h^{-1}$) considering a boundary layer height of 1000 m and hence is negligible.

3.3.3 HONO formation by nitric acid photolysis

Adsorbed HNO_3 on humid surfaces Reaction (R9) seems to be more rapidly photolyzed than HNO_3 in the gas phase or in aqueous solution (Zhou et al., 2003; Abida et al., 2012). Therefore, leaves and needles loaded with nitric acid could be a major source of HONO in clean environments (Zhou et al., 2011). This mechanism has also been postulated as significant for the boreal forest by Raivonen et al. (2006) to explain light induced NO_y (NO, NO_2, HONO, HNO_3, peroxy acyl nitrate) emissions. To estimate the

strength of this source we used a constant surface loading of HNO_3 of $(8.3 \pm 3.1) \times 10^{-5}$ mol m^{-2} (Zhou et al., 2011). The gas phase photolysis frequency for HNO_3 was parameterized using $J(NO_2)$ and $J(O^1D)$ (Sander et al., 2011). By adsorbing to the surface the absorption cross-sections of HNO_3 increases (Zhu et al., 2010; Abida et al., 2012), which is typically considered by the use of an empirical enhancement factor for natural systems (Zhou et al., 2011; Li et al., 2012). For Fig. 7 we used the enhancement factor of 43 (Zhou et al., 2003, 2011).

The photolysis rate of surface adsorbed HNO_3 needs to be more than 400 times enhanced compared to the photolysis in gas phase to explain $P_{unknown}$ of HONO (Fig. 7). The error of $P_{HNO_{3(ads)}}$ was calculated by using the standard error of the surface loading of HNO_3 (Zhou et al., 2011). $J(HNO_3)$ constitutes the only variable of $P_{HNO_{3(ads)}}$ and is closely correlated to $J(NO_2)$ and $J(O^1D)$. This leads to a similar correlation of $P_{unknown}$ with $P_{HNO_{3(ads)}}$, like seen before with $J(NO_2)$ (Fig. 6). An additional correlation might derive from the mechanism of HNO_3 photolysis, which is not fully understood by now. Zhou et al. (2011) proposed that formed NO_2 during HNO_3 photolysis reacts further with organics on the surface to form HONO Reaction (R6) as proposed by Stemmler et al. (2006).

3.4 Direct comparison of $P_{unknown}$ determined for two different heights

The ratio of $J(NO_2)$ at 24 m to $J(NO_2)$ at 2 m tracks the ratio of direct and diffuse radiation penetrating the canopy. In the early morning the ratio increases, due to increasing direct sunlight at the upper height. With the rising sun more direct sunlight penetrates the canopy and a rather constant ratio develops which seems to be influenced by light patches. The ratio of $P_{unknown}$ at 24 m to $P_{unknown}$ at 1 m during daytime is mainly above 1, except for the first value where $P_{unknown}$ at both heights were still negative (Fig. 5). It strongly decreases from values above 4 in the morning hours before it gets more stable with values around 2, but still decreases until 2 h after reaching the minimum of solar zenith angle ($\sim 43^\circ$). This diel pattern can be explained by a combination of two

processes; the change of the photolysis frequency and the change of the concentration gradient (Fig. 8a). The product of both, the concentration and the photolysis frequency equals the photolytic loss rate, L_{phot}, which is the unbalanced sink that determines $P_{unknown}$ (see Figs. 5, 8b and c). This is at least valid from 8:30 to 17:30 where the contribution of other source and sink terms is less than 20 %. The HONO concentrations above the canopy are higher than below the canopy in the morning (values over unity in Fig. 8a). The gradients vary around zero from late morning to noon and in the afternoon the concentrations below the canopy are higher. This closely resembles the pattern found by Sörgel et al. (2011b) for a different forest ecosystem and might therefore be typical for forests in general. Sörgel et al. (2011b) showed that this could be attributed to different sources and sinks and the extent of the vertical exchange between the forest and the atmosphere above. However, the variability of the ratios is smallest at minimum solar zenith angle, which is the maximum of $J(HONO)$. In a strict sense this is the only period where the budget could be used for the determination of $P_{unknown}$ as the assumptions like well mixed conditions (i.e. no concentration gradients), stationarity due to low lifetime of HONO and potentially establishment of a PSS are fulfilled. During this period it could be questioned if a budget below canopy makes sense as the portion below canopy where $J(HONO)$ and thus L_{phot} is reduced is very small compared to the whole boundary layer and recombination of NO and OH below canopy has been found to play a minor role (Sect. 3.2).

Impressively, $P_{unknown}$ correlates much better with L_{phot} (Fig. 8b and c) than with $J(NO_2)$ or with the ratio of $J(NO_2)$ to concentration of NO_2 (Fig. 6). This correlation is not disturbed by any environmental condition, like the different regimes of stressed and normal boreal and even more astonishing it is not disturbed by the wild fire pollution plumes transported from Russia (Nölscher et al., 2012), since the corresponding data points are included. The almost perfect correlation of $P_{unknown}$ with L_{phot} is caused by the low contribution to the budget of all other processes (sources and sinks) considered so far. Even including the parameterized HNO_3 photolysis (Sect. 3.4.3) would not change much as it is only around 10 % of $P_{unknown}$. Therefore, the unknown source is

a process that exactly balances HONO photolysis or the sink itself is erroneous. Nevertheless, this unbalanced photolysis term ($P_{unknown}$) has been found by applying different techniques for HONO detection such as LOPAP (e.g., Kleffmann et al., 2005; Sörgel et al., 2011a), denuder (Acker et al., 2006), differential optical absorption spectroscopy (Alicke et al., 2002; Wong et al., 2012) and recently by using chemical ionization mass spectrometry (VandenBoer et al., 2013). Additionally, recent flux measurements reported strong daytime upward fluxes of HONO (Zhou et al., 2011; Ren et al., 2011), thus confirming a ground source of HONO.

4 Conclusion

Concentrations of HONO during daytime exceeded on average the expected values calculated by the PSS by a factor of about 20 and thus lead to an imbalanced budget above and below canopy. To balance the budget an additional yet unknown source is required. However, photolysis of ortho-nitrophenols is likely of minor importance under the clean environment of the boreal forest. A laboratory measurement of a soil sample in a dynamic chamber shows that direct soil emissions of HONO are insignificant for the measurement site in the boreal forest, featuring low soil nutrient content and low soil pH. However, the photolytically active radiation has a major influence on the budget of HONO, since the missing source resembles the photolytic loss of HONO by day. It was not possible to clearly identify the most important source term, but a tendency for a possible coupling of different processes is most likely. E.g. the photolytic dissociation of HNO_3 adsorbed on humid surfaces and the conversion of NO_2 on photolytically activated surfaces, like humic acids, might occur simultaneously. However, the almost perfect correlation of $P_{unknown}$ with L_{phot} is caused by the low contribution of the considered processes to the budget and hence, the unknown source is a process that exactly balances HONO photolysis. Further investigations in the field are needed to understand daytime HONO chemistry and its implication to the budget. Especially the role of vertical mixing needs to be analysed in more detail.

Acknowledgements. This project was funded by the Max Planck Society. The work was supported by the Max Planck Graduate Center with the Johannes Gutenberg University Mainz (MPGC). The entire HUMPPA-COPEC team is grateful for the support of the Hyytiälä site engineers and staff. We like to thank for the support of the European Community Research Infrastructure Action under the FP6 "Structuring the European Research Area" Programme, EUSAAR 15 Contract No. RII3-CT-2006-026140. The campaign measurements and analyses were supported by the ERC Grant ATMNUCLE (project No. 227463), Academy of Finland Center of Excellence program (project No. 1118615), The European Integrated project on Aerosol Cloud Climate and Air Quality Interactions EUCAARI (project No. 036833-2), the EUSAAR TNA (project No. 400586), and the IMECC TA (project No. 4006261). We also wish to thank C. Breitenberger, J. Crowley, T. Klüpfel, U. Parchatka, M. Rudolf, L. Ganzeveld for their support during HUMPPA-COPEC 2010. We are further grateful to S. Hohlmann, M. Welling, D. Plake, A. Moravek, E. Falge, T. Behrendt, D. Mogensen for supporting the measurements and for the fruitful discussions.

The service charges for this open access publication
have been covered by the Max Planck Society.

References

Abida, O., Du, J., and Zhu, L.: Investigation of the photolysis of the surface-adsorbed HNO_3 by combining laser photolysis with Brewster angle cavity ring-down spectroscopy, Chem. Phys. Lett., 534, 77–82, doi:10.1016/j.cplett.2012.03.034, 2012.

Acker, K., Möller, D., Wieprecht, W., Meixner, F. X., Bohn, B., Gilge, S., Plass-Dülmer, C., and Berresheim, H.: Strong daytime production of OH from HNO_2 at a rural mountain site, Geophys. Res. Lett., 33, L02809, doi:10.1029/2005GL024643, 2006.

Alicke, B., Platt, U., and Stutz, J.: Impact of nitrous acid photolysis on the total hydroxyl radical budget during the limitation of oxidant production/Pianura Padana Produzione di Ozono study in Milan, J. Geophys. Res., 107, LOP9-1-LOP9-LOP9-17, doi:10.1029/2000jd000075, 2002.

Atkinson, R., Baulch, D. L., Cox, R. A., Crowley, J. N., Hampson, R. F., Hynes, R. G., Jenkin, M. E., Rossi, M. J., and Troe, J.: Evaluated kinetic and photochemical data for at-

mospheric chemistry: Volume I – gas phase reactions of O_x, HO_x, NO_x and SO_x species, Atmos. Chem. Phys., 4, 1461–1738, doi:10.5194/acp-4-1461-2004, 2004.
Aubin, D. G. and Abbatt, J. P. D.: Interaction of NO_2 with hydrocarbon soot: focus on HONO yield, surface modification, and mechanism, J. Phys. Chem. A, 111, 6263–6273, 2007.
Baergen, A. M. and Donaldson, D. J.: Photochemical renoxification of nitric acid on real urban grime, Environ. Sci. Technol., 47, 815–820, doi:10.1021/es3037862, 2013.
Bejan, I., Abd El Aal, Y., Barnes, I., Benter, T., Bohn, B., Wiesen, P., and Kleffmann, J.: The photolysis of ortho-nitrophenols: a new gas phase source of HONO, Phys. Chem. Chem. Phys., 8, 2028–2035, 2006.
Bohn, B., Corlett, G. K., Gillmann, M., Sanghavi, S., Stange, G., Tensing, E., Vrekoussis, M., Bloss, W. J., Clapp, L. J., Kortner, M., Dorn, H.-P., Monks, P. S., Platt, U., Plass-Dülmer, C., Mihalopoulos, N., Heard, D. E., Clemitshaw, K. C., Meixner, F. X., Prevot, A. S. H., and Schmitt, R.: Photolysis frequency measurement techniques: results of a comparison within the ACCENT project, Atmos. Chem. Phys., 8, 5373–5391, doi:10.5194/acp-8-5373-2008, 2008.
Conrad, R.: Soil microorganisms as controllers of atmospheric trace gases (H_2, CO, CH_4, OCS, N_2O, and NO), Microbiol. Rev., 60, 609–640, 1996.
De Jesus Medeiros, D. and Pimentel, A. S.: New insights in the atmospheric HONO formation: new pathways for N_2O_4 isomerization and NO_2 dimerization in the presence of water, J. Phys. Chem. A, 115, 6357–6365, 2011.
Elshorbany, Y. F., Steil, B., Brühl, C., and Lelieveld, J.: Impact of HONO on global atmospheric chemistry calculated with an empirical parameterization in the EMAC model, Atmos. Chem. Phys., 12, 9977–10000, doi:10.5194/acp-12-9977-2012, 2012.
Finlayson-Pitts, B. J., Wingen, L. M., Sumner, A. L., Syomin, D., and Ramazan, K. A.: The heterogeneous hydrolysis of NO_2 in laboratory systems and in outdoor and indoor atmospheres: an integrated mechanism, Phys. Chem. Chem. Phys., 5, 223–242, doi:10.1039/b208564j, 2003.
Goodman, A. L., Bernard, E. T., and Grassian, V. H.: Spectroscopic study of nitric acid and water adsorption on oxide particles: enhanced nitric acid uptake kinetics in the presence of adsorbed water, J. Phys. Chem. A, 105, 6443–6457, doi:10.1021/jp003722l, 2001.
Harrison, R. M., Peak, J. D., and Collins, G. M.: Tropospheric cycle of nitrous acid, J. Geophys. Res.-Atmos., 101, 14429–14439, 1996.

Heland, J., Kleffmann, J., Kurtenbach, R., and Wiesen, P.: A new instrument to measure gaseous nitrous acid (HONO) in the atmosphere, Environ. Sci. Technol., 35, 3207–3212, doi:10.1021/es000303t, 2001.
Hens, K., Novelli, A., Martinez, M., Auld, J., Axinte, R., Bohn, B., Fischer, H., Keronen, P., Kubistin, D., Nölscher, A. C., Oswald, R., Paasonen, P., Petäjä, T., Regelin, E., Sander, R., Sinha, V., Sipilä, M., Taraborrelli, D., Tatum Ernest, C., Williams, J., Lelieveld, J., and Harder, H.: Observation and modelling of HO_x radicals in a boreal forest, Atmos. Chem. Phys. Discuss., 13, 28561–28629, doi:10.5194/acpd-13-28561-2013, 2013.
Hosaynali Beygi, Z., Fischer, H., Harder, H. D., Martinez, M., Sander, R., Williams, J., Brookes, D. M., Monks, P. S., and Lelieveld, J.: Oxidation photochemistry in the Southern Atlantic boundary layer: unexpected deviations of photochemical steady state, Atmos. Chem. Phys., 11, 8497–8513, doi:10.5194/acp-11-8497-2011, 2011.
Junninen, H., Lauri, A., Keronen, P., Aalto, P., Hiltunen, V., Hari, P., and Kulmala, M.: Smart-SMEAR: on-line data exploration and visualization tool for SMEAR stations., Boreal Environ. Res., 14, 447–457, 2009.
Kleffmann, J.: Daytime sources of nitrous acid (HONO) in the atmospheric boundary layer, Chem. Phys. Chem., 8, 1137–1144, 2007.
Kleffmann, J., Heland, J., Kurtenbach, R., Lörzer, J., and Wiesen, P.: A new instrument (LOPAP) for the detection of nitrous acid (HONO), Environ. Sci. Pollut. R., 4, 48–54, 2002.
Kleffmann, J., Kurtenbach, R., Lörzer, J., Wiesen, P., Kalthoff, N., Vogel, B., and Vogel, H.: Measured and simulated vertical profiles of nitrous acid – Part I: Field measurements, Atmos. Environ., 37, 2949–2955, doi:10.1016/s1352-2310(03)00242-5, 2003.
Kleffmann, J., Gavriloaiei, T., Hofzumahaus, A., Holland, F., Koppmann, R., Rupp, L., Schlosser, E., Siese, M., and Wahner, A.: Daytime formation of nitrous acid: a major source of OH radicals in a forest, Geophys. Res. Lett., 32, L05818 doi:10.1029/2005GL022524, 2005.
Korhonen, J. F. J., Pihlatie, M., Pumpanen, J., Aaltonen, H., Hari, P., Levula, J., Kieloaho, A.-J., Nikinmaa, E., Vesala, T., and Ilvesniemi, H.: Nitrogen balance of a boreal Scots pine forest, Biogeosciences, 10, 1083–1095, doi:10.5194/bg-10-1083-2013, 2013.
Kourtchev, I., Fuller, S., Aalto, J., Ruuskanen, T. M., McLeod, M. W., Maenhaut, W., Jones, R., Kulmala, M., and Kalberer, M.: Molecular composition of boreal forest aerosol from Hyytiala, Finland, using ultrahigh resolution mass spectrometry, Environ. Sci. Technol., 47, 4069–4079, doi:10.1021/es3051636, 2013.

Kraus, A. and Hofzumahaus, A.: Field measurements of atmospheric photolysis frequencies for O_3, NO_2, HCHO, CH_3CHO, H_2O_2, and HONO by UV spectroradiometry, J. Atmos. Chem., 31, 161–180, 1998.

Kubota, M. and Asami, T.: Volatilization of nitrous-acid from upland soils, Soil Sci. Plant Nutr., 31, 27–34, 1985.

Lammel, G. and Cape, J. N.: Nitrous acid and nitrite in the atmosphere, Chem. Soc. Rev., 25, 361–369, 1996.

Lee, B. H., Wood, E. C., Herndon, S. C., Lefer, B. L., Luke, W. T., Brune, W. H., Nelson, D. D., Zahniser, M. S., and Munger, J. W.: Urban measurements of atmospheric nitrous acid: a caveat on the interpretation of the HONO photostationary state, J. Geophys. Res.-Atmos., 118, 12274–12281, doi:10.1002/2013JD020341, 2013.

Li, X., Brauers, T., Häseler, R., Bohn, B., Fuchs, H., Hofzumahaus, A., Holland, F., Lou, S., Lu, K. D., Rohrer, F., Hu, M., Zeng, L. M., Zhang, Y. H., Garland, R. M., Su, H., Nowak, A., Wiedensohler, A., Takegawa, N., Shao, M., and Wahner, A.: Exploring the atmospheric chemistry of nitrous acid (HONO) at a rural site in Southern China, Atmos. Chem. Phys., 12, 1497–1513, doi:10.5194/acp-12-1497-2012, 2012.

Maljanen, M., Yli-Pirilä, P., Hytönen, J., Joutsensaari, J., and Martikainen, P. J.: Acidic northern soils as sources of atmospheric nitrous acid (HONO), Soil Biol. Biochem., 67, 94–97, doi:10.1016/j.soilbio.2013.08.013, 2013.

Monge, M. E., D'Anna, B., Mazri, L., Giroir-Fendler, A., Ammann, M., Donaldson, D. J., and George, C.: Light changes the atmospheric reactivity of soot, P. Natl. Acad. Sci. USA, 107, 6605–6609, doi:10.1073/pnas.0908341107, 2010.

Nölscher, A. C., Williams, J., Sinha, V., Custer, T., Song, W., Johnson, A. M., Axinte, R., Bozem, H., Fischer, H., Pouvesle, N., Phillips, G., Crowley, J. N., Rantala, P., Rinne, J., Kulmala, M., Gonzales, D., Valverde-Canossa, J., Vogel, A., Hoffmann, T., Ouwersloot, H. G., de Arellano, J. V. G., and Lelieveld, J.: Summertime total OH reactivity measurements from boreal forest during HUMPPA-COPEC 2010, Atmos. Chem. Phys., 12, 8257–8270, doi:10.5194/acp-12-8257-2012, 2012.

Novelli, A., Hens, K., Tatum Ernest, C., Kubistin, D., Regelin, E., Elste, T., Plass-Dülmer, C., Martinez, M., Lelieveld, J., and Harder, H.: Characterisation of an inlet pre-injector laser induced fluorescence instrument for the measurement of ambient hydroxyl radicals, Atmos. Meas. Tech. Discuss., 7, 819–858, doi:10.5194/amtd-7-819-2014, 2014.

Oswald, R., Behrendt, T., Ermel, M., Wu, D., Su, H., Cheng, Y., Breuninger, C., Moravek, A., Mougin, E., Delon, C., Loubet, B., Pommerening-Röser, A., Sorgel, M., Pöschl, U., Hoffmann, T., Andreae, M. O., Meixner, F. X., and Trebs, I.: HONO emissions from soil bacteria as a major source of atmospheric reactive nitrogen, Science, 341, 1233–1235, doi:10.1126/science.1242266, 2013.

Ouwersloot, H. G., Vilà-Guerau de Arellano, J., Nölscher, A. C., Krol, M. C., Ganzeveld, L. N., Breitenberger, C., Mammarella, I., Williams, J., and Lelieveld, J.: Characterization of a boreal convective boundary layer and its impact on atmospheric chemistry during HUMPPA-COPEC-2010, Atmos. Chem. Phys., 12, 9335–9353, doi:10.5194/acp-12-9335-2012, 2012.

Park, J. Y. and Lee, Y. N.: Solubility and decomposition kinetics of nitrous-acid in aqueous-solution, J. Phys. Chem., 92, 6294–6302, doi:10.1021/j100333a025, 1988.

Perner, D. and Platt, U.: Detection of nitrous-acid in the atmosphere by differential optical-absorption, Geophys. Res. Lett., 6, 917–920, doi:10.1029/GL006i012p00917, 1979.

Petäjä, T., Mauldin, III, R. L., Kosciuch, E., McGrath, J., Nieminen, T., Paasonen, P., Boy, M., Adamov, A., Kotiaho, T., and Kulmala, M.: Sulfuric acid and OH concentrations in a boreal forest site, Atmos. Chem. Phys., 9, 7435–7448, doi:10.5194/acp-9-7435-2009, 2009.

Raivonen, M., Bonn, B., Sanz, M. J., Vesala, T., Kulmala, M., and Hari, P.: UV-induced NO_y emissions from Scots pine: could they originate from photolysis of deposited HNO_3?, Atmos. Environ., 40, 6201–6213, doi:10.1016/j.atmosenv.2006.03.063, 2006.

Ramazan, K. A., Syomin, D., and Finlayson-Pitts, B. J.: The photochemical production of HONO during the heterogeneous hydrolysis of NO_2, Phys. Chem. Chem. Phys., 6, 3836–3843, 2004.

Ren, X., Sanders, J. E., Rajendran, A., Weber, R. J., Goldstein, A. H., Pusede, S. E., Browne, E. C., Min, K.-E., and Cohen, R. C.: A relaxed eddy accumulation system for measuring vertical fluxes of nitrous acid, Atmos. Meas. Tech., 4, 2093–2103, doi:10.5194/amt-4-2093-2011, 2011.

Rohrer, F. and Berresheim, H.: Strong correlation between levels of tropospheric hydroxyl radicals and solar ultraviolet radiation, Nature, 442, 184–187, doi:10.1038/nature04924, 2006.

Rummel, U., Ammann, C., Gut, A., Meixner, F. X., and Andreae, M. O.: Eddy covariance measurements of nitric oxide flux within an Amazonian rain forest, J. Geophys. Res., 107, 8050, doi:10.1029/2001JD000520, 2002.

Sander, S. P., Abbatt, J. P. D., Barker, J. R., Burkholder, J. B., Friedl, R. R., Golden, D. M., Huie, R. E., Kolb, C. E., Kurylo, M. J., Moortgat, G. K., Orkin, V. L., and Wine, P. H.: Chemical

Kinetics and Photochemical Data for Use in Atmospheric Studies, Evaluation No. 17, in: JPL Publication 10-6, Jet Propulsion Laboratory, Pasadena, 2011.

Skopp, J., Jawson, M. D., and Doran, J. W.: Steady-state aerobic microbial activity as a function of soil-water content, Soil Sci. Soc. Am. J., 54, 1619–1625, 1990.

Sörgel, M., Regelin, E., Bozem, H., Diesch, J.-M., Drewnick, F., Fischer, H., Harder, H., Held, A., Hosaynali-Beygi, Z., Martinez, M., and Zetzsch, C.: Quantification of the unknown HONO daytime source and its relation to NO_2, Atmos. Chem. Phys., 11, 10433–10447, doi:10.5194/acp-11-10433-2011, 2011a.

Sörgel, M., Trebs, I., Serafimovich, A., Moravek, A., Held, A., and Zetzsch, C.: Simultaneous HONO measurements in and above a forest canopy: influence of turbulent exchange on mixing ratio differences, Atmos. Chem. Phys., 11, 841–855, doi:10.5194/acp-11-841-2011, 2011b.

Sörgel, M., Wu, D., Trebs, I., and Held, A.: Sources and sinks of HONO in a heterogeneous forest landscape, in preparation, 2014.

Stemmler, K., Ammann, M., Donders, C., Kleffmann, J., and George, C.: Photosensitized reduction of nitrogen dioxide on humic acid as a source of nitrous acid, Nature, 440, 195–198, 2006.

Stemmler, K., Ndour, M., Elshorbany, Y., Kleffmann, J., D'Anna, B., George, C., Bohn, B., and Ammann, M.: Light induced conversion of nitrogen dioxide into nitrous acid on submicron humic acid aerosol, Atmos. Chem. Phys., 7, 4237–4248, doi:10.5194/acp-7-4237-2007, 2007.

Su, H., Cheng, Y. F., Cheng, P., Zhang, Y. H., Dong, S., Zeng, L. M., Wang, X., Slanina, J., Shao, M., and Wiedensohler, A.: Observation of nighttime nitrous acid (HONO) formation at a non-urban site during PRIDE-PRD2004 in China, Atmos. Environ., 42, 6219–6232, doi:10.1016/j.atmosenv.2008.04.006, 2008a.

Su, H., Cheng, Y. F., Min, S., Dong Feng, G., Zhong Ying, Y., Li Min, Z., Slanina, J., Yuan Hang, Z., and Wiedensohler, A.: Nitrous acid (HONO) and its daytime sources at a rural site during the 2004 PRIDE-PRD experiment in China, J. Geophys. Res.-Atmos., 114, D14312, doi:10.1029/2007jd009060, 2008b.

Su, H., Cheng, Y. F., Shao, M., Gao, D. F., Yu, Z. Y., Zeng, L. M., Slanina, J., Zhang, Y. H., and Wiedensohler, A.: Nitrous acid (HONO) and its daytime sources at a rural site during the 2004 PRIDE-PRD experiment in China, J. Geophys. Res.-Atmos., 113, D14312, doi:10.1029/2007jd009060, 2008c.

Su, H., Cheng, Y., Oswald, R., Behrendt, T., Trebs, I., Meixner, F. X., Andreae, M. O., Cheng, P., Zhang, Y., and Pöschl, U.: Soil Nitrite as a Source of Atmospheric HONO and OH Radicals, Science, 333, 1616–1618, doi:10.1126/science.1207687, 2011.

Trebs, I., Bohn, B., Ammann, C., Rummel, U., Blumthaler, M., Königstedt, R., Meixner, F. X., Fan, S., and Andreae, M. O.: Relationship between the NO_2 photolysis frequency and the solar global irradiance, Atmos. Meas. Tech., 2, 725–739, doi:10.5194/amt-2-725-2009, 2009.

Twigg, M. M., House, E., Thomas, R., Whitehead, J., Phillips, G. J., Famulari, D., Fowler, D., Gallagher, M. W., Cape, J. N., Sutton, M. A., and Nemitz, E.: Surface/atmosphere exchange and chemical interactions of reactive nitrogen compounds above a manured grassland, Agr. Forest Meteorol., 151, 1488–1503, doi:10.1016/j.agrformet.2011.06.005, 2011.

VandenBoer, T. C., Brown, S. S., Murphy, J. G., Keene, W. C., Young, C. J., Pszenny, A. A. P., Kim, S., Warneke, C., de Gouw, J. A., Maben, J. R., Wagner, N. L., Riedel, T. P., Thornton, J. A., Wolfe, D. E., Dubé, W. P., Öztürk, F., Brock, C. A., Grossberg, N., Lefer, B., Lerner, B., Middlebrook, A. M., and Roberts, J. M.: Understanding the role of the ground surface in HONO vertical structure: high resolution vertical profiles during NACHTT-11, J. Geophys. Res.-Atmos., 118, 10155–10171, doi:10.1002/jgrd.50721, 2013.

Williams, J., Crowley, J., Fischer, H., Harder, H., Martinez, M., Petäjä, T., Rinne, J., Bäck, J., Boy, M., Dal Maso, M., Hakala, J., Kajos, M., Keronen, P., Rantala, P., Aalto, J., Aaltonen, H., Paatero, J., Vesala, T., Hakola, H., Levula, J., Pohja, T., Herrmann, F., Auld, J., Mesarchaki, E., Song, W., Yassaa, N., Nölscher, A., Johnson, A. M., Custer, T., Sinha, V., Thieser, J., Pouvesle, N., Taraborrelli, D., Tang, M. J., Bozem, H., Hosaynali-Beygi, Z., Axinte, R., Oswald, R., Novelli, A., Kubistin, D., Hens, K., Javed, U., Trawny, K., Breitenberger, C., Hidalgo, P. J., Ebben, C. J., Geiger, F. M., Corrigan, A. L., Russell, L. M., Ouwersloot, H. G., Vilà-Guerau de Arellano, J., Ganzeveld, L., Vogel, A., Beck, M., Bayerle, A., Kampf, C. J., Bertelmann, M., Köllner, F., Hoffmann, T., Valverde, J., González, D., Riekkola, M.-L., Kulmala, M., and Lelieveld, J.: The summertime Boreal forest field measurement intensive (HUMPPA-COPEC-2010): an overview of meteorological and chemical influences, Atmos. Chem. Phys., 11, 10599–10618, doi:10.5194/acp-11-10599-2011, 2011.

Wong, K. W., Tsai, C., Lefer, B., Haman, C., Grossberg, N., Brune, W. H., Ren, X., Luke, W., and Stutz, J.: Daytime HONO vertical gradients during SHARP 2009 in Houston, TX, Atmos. Chem. Phys., 12, 635–652, doi:10.5194/acp-12-635-2012, 2012.

Wong, K. W., Tsai, C., Lefer, B., Grossberg, N., and Stutz, J.: Modeling of daytime HONO vertical gradients during SHARP 2009, Atmos. Chem. Phys., 13, 3587–3601, doi:10.5194/acp-13-3587-2013, 2013.

Yabushita, A., Enami, S., Sakamoto, Y., Kawasaki, M., Hoffmann, M. R., and Colussi, A. J.: Anion-catalyzed dissolution of NO_2 on aqueous microdroplets, J. Phys. Chem. A, 113, 4844–4848, doi:10.1021/jp900685f, 2009.

York, D., Evensen, N. M., Martìnez, M. L., and De Basabe Delgado, J.: Unified equations for the slope, intercept, and standard errors of the best straight line, Am. J. Phys., 72, 367–375, doi:10.1119/1.1632486, 2004.

Zhang, N., Zhou, X., Bertman, S., Tang, D., Alaghmand, M., Shepson, P. B., and Carroll, M. A.: Measurements of ambient HONO concentrations and vertical HONO flux above a northern Michigan forest canopy, Atmos. Chem. Phys., 12, 8285–8296, doi:10.5194/acp-12-8285-2012, 2012.

Zhou, X. L., Gao, H. L., He, Y., Huang, G., Bertman, S. B., Civerolo, K., and Schwab, J.: Nitric acid photolysis on surfaces in low-NO_x environments: significant atmospheric implications, Geophys. Res. Lett., 30, 2217 doi:10.1029/2003gl018620, 2003.

Zhou, X. L., Zhang, N., TerAvest, M., Tang, D., Hou, J., Bertman, S., Alaghmand, M., Shepson, P. B., Carroll, M. A., Griffith, S., Dusanter, S., and Stevens, P. S.: Nitric acid photolysis on forest canopy surface as a source for tropospheric nitrous acid, Nat. Geosci., 4, 440–443, doi:10.1038/ngeo1164, 2011.

Zhu, C., Xiang, B., Zhu, L., and Cole, R.: Determination of absorption cross sections of surface-adsorbed HNO_3 in the 290–330 nm region by Brewster angle cavity ring-down spectroscopy, Chem. Phys. Lett., 458, 373–377, doi:10.1016/j.cplett.2008.04.125, 2008.

Zhu, C. Z., Xiang, B., Chu, L. T., and Zhu, L.: 308 nm photolysis of nitric acid in the gas phase, on aluminum surfaces, and on ice films, J. Phys. Chem. A, 114, 2561–2568, doi:10.1021/jp909867a, 2010.

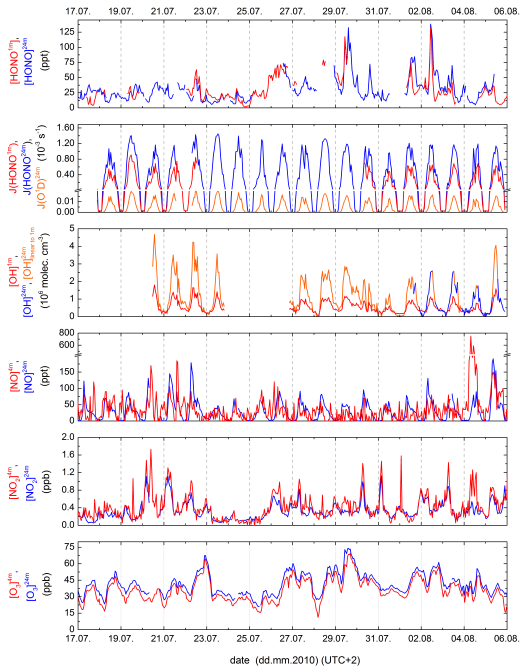

Fig. 1. Overview of the measured concentration of different trace gases and the photolysis frequencies J(HONO) and $J(O^1D)$. The linearly connected data points represent 60 min average values. Mixing ratios or concentrations are shown for the period where HONO was measured at both heights. $[OH]^{24\,m}_{\text{linear to }1\,m}$ was used to fill the gaps in OH measurements above the canopy (see Fig. 2a).

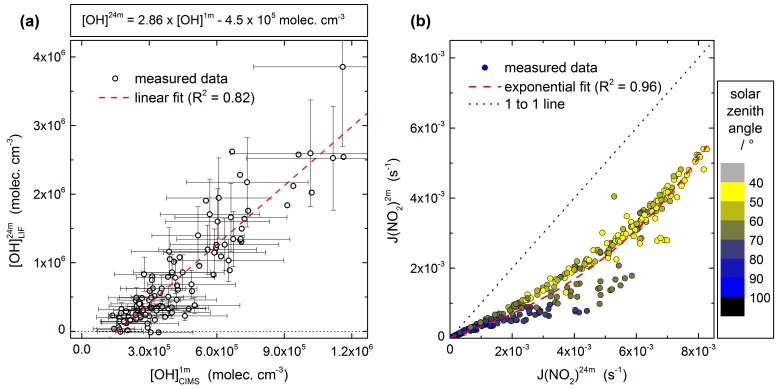

Fig. 2. (a) The linear correlation of OH concentration below and above the canopy was used for interpolating data of OH concentration above the canopy. **(b)** Similar to **(a)** the exponential correlation of measured photolysis frequency below and above the canopy was used to interpolate data of $J(NO_2)$ below the canopy. Color code of dots represents the solar zenith angle. Additionally the 1 to 1 line is shown as dashed line.

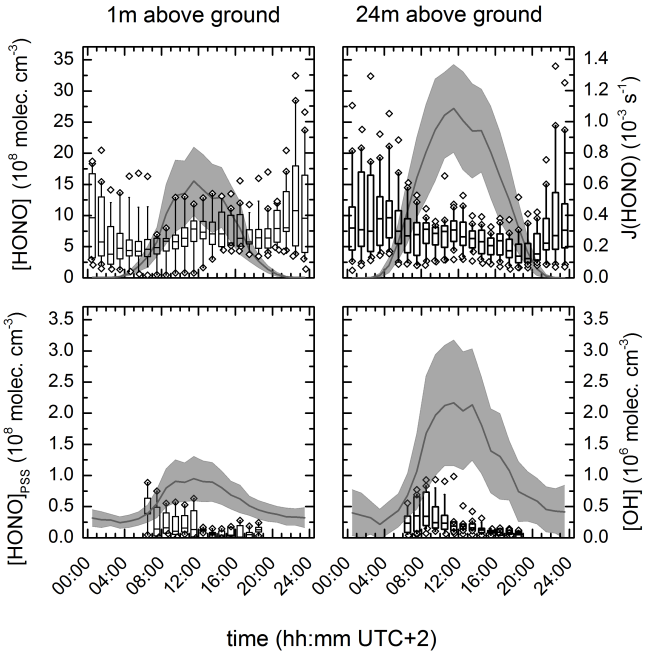

Fig. 3. Upper panels show box plots of the diel cycle of HONO measured at 1 m and 24 m, respectively and the average corresponding $J(HONO)$ with standard deviation (grey shaded line). Lower panels show box plots for the calculated PSS concentration of HONO for the heights of 1 m and 24 m, respectively, during daytime (lifetime of HONO below 4 h) where PSS is possibly attained. Additionally, the average concentration of OH with standard deviation (grey shaded line) for the two respective heights is presented. The boxes represent the 25 to 75 percentile, the line within the box is the median, the bars show the 10 to 90 percentile and outliers are marked as open diamonds.

Discussion Paper | Discussion Paper | Discussion Paper | Discussion Paper |

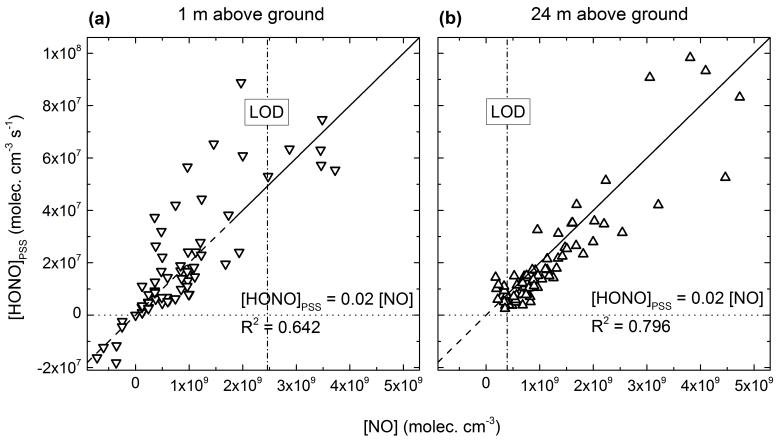

Fig. 4. The PSS concentration of HONO, $[HONO]_{PSS}$, at 1 m measurement height **(a)** and at 24 m measurement height **(b)** is plotted against the concentration of NO at the corresponding heights. The dashed-dotted vertical line reflects the lower limit of detection (LOD) for each NO measurement. The linear fit using a fixed slope of 0.02 and no offset leads to a reasonable correlations between $[HONO]_{PSS}$ and [NO] in both cases.

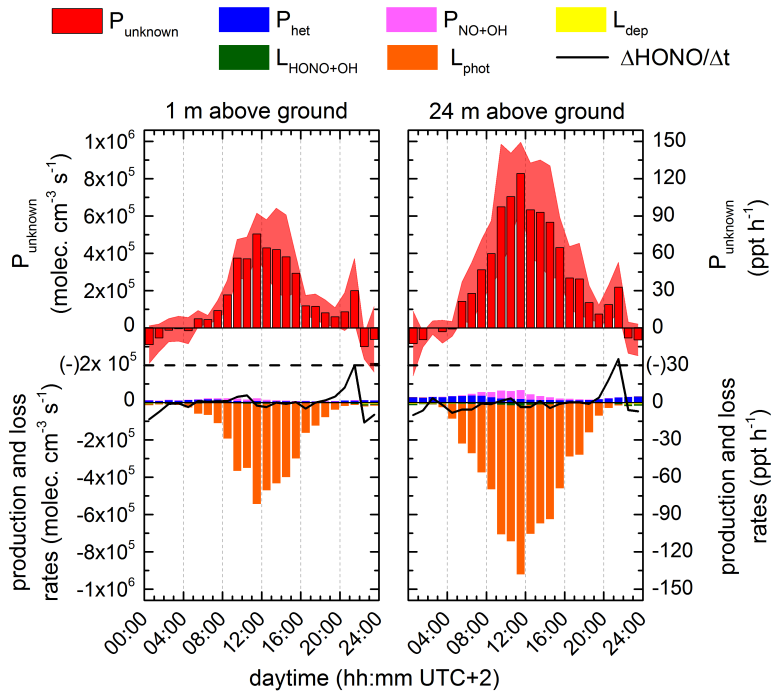

Fig. 5. The diel variation of $P_{unknown}$ (red bars, upper panel) with standard deviation (red shade) and single production and loss terms (lower panel) for the two heights are shown. The scales and units at the left and right hand y-axis are valid for both measurement heights and were chosen for an easy comparison with other publications.

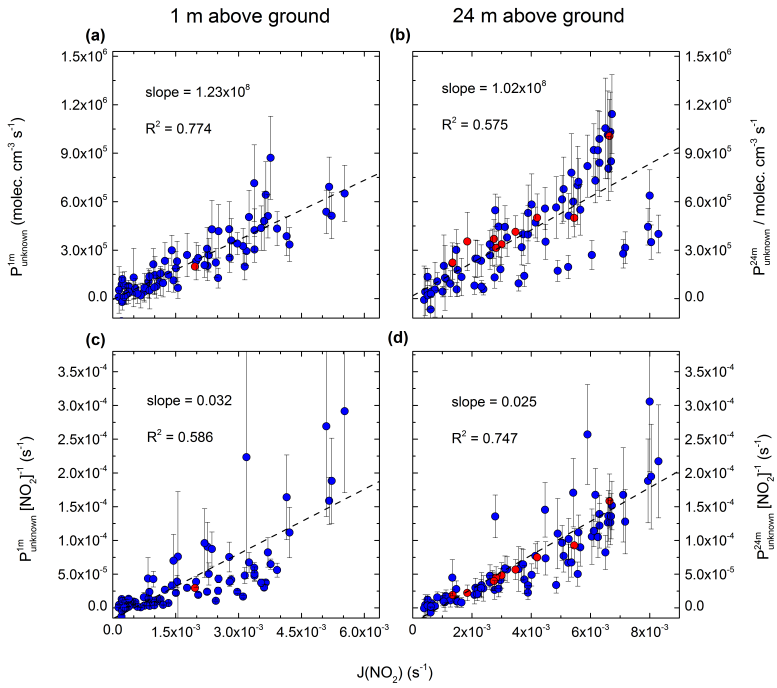

Fig. 6. In the upper panels, (**a** and **b**), P_{unknown} for both measurement heights is linearly correlated with corresponding $J(NO_2)$. In the lower panels, (**c** and **d**), P_{unknown} is scaled by the NO_2 concentration and still linearly correlated with $J(NO_2)$. Blue dots denote budget data availability at both heights, whereas red dots are available only at the respective measurement height. Linear fits refer to total data available (blue and red).

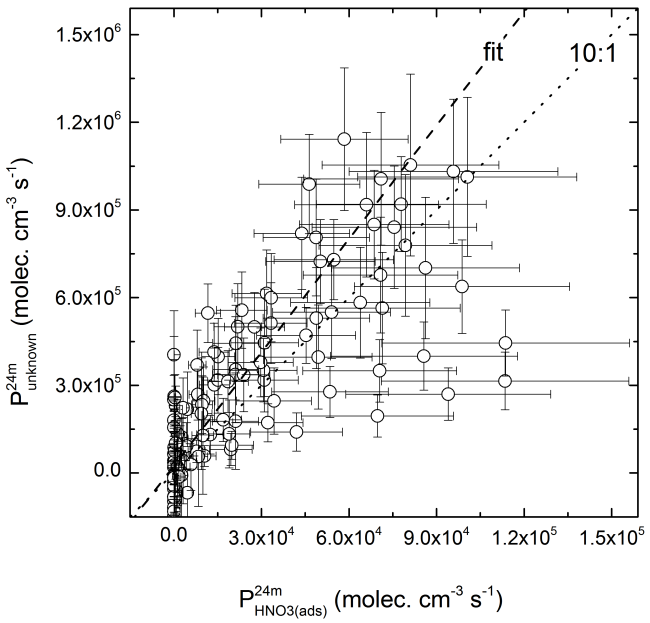

Fig. 7. P_{unknown} at the measurement height of 24 m during daytime is plotted against the production of HONO from photolysis of adsorbed HNO_3 on leaf surfaces, $P_{HNO_{3(ads)}}$. With an enhancement factor of 43 and a surface loading of $(8.3 \pm 3.1) \times 10^{-5}$ mol m^{-2} it might explain up to 10 % of P_{unknown}, indicated by the 10 to 1 line (dotted line). The York linear fit (York et al., 2004) yields in $P_{\mathrm{unknown}} = (12.9 \pm 1.0) \times P_{HNO_{3(ads)}} + (2.4 \pm 1.1) \times 10^4$ molecules cm^{-3} s^{-1}.

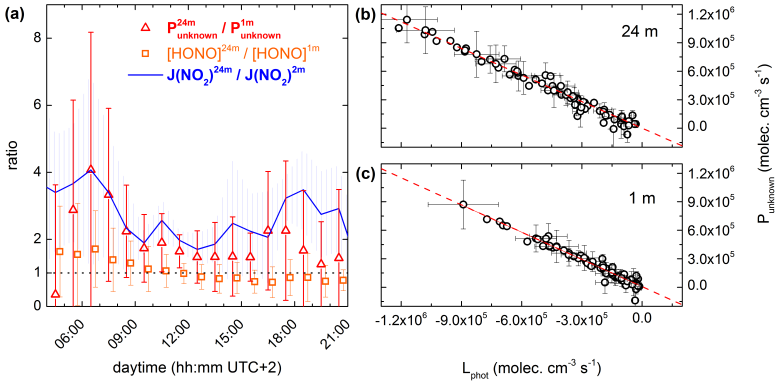

Fig. 8. (a) The average ratio of $P^{24\,m}_{unknown}$ to $P^{1\,m}_{unknown}$ (red triangles), the average ratio of $[HONO]^{24\,m}$ to $[HONO]^{1\,m}$ (orange squares) and the average ratio of $J(NO_2)^{24\,m}$ to $J(NO_2)^{2\,m}$ (blue line) change during daytime (lifetime of HONO < 4 h). For clarity a second x-coordinate for the ratio of $[HONO]^{24\,m}$ to $[HONO]^{1\,m}$ is used with a shift of +15 min, but is not shown. **(b)** $P^{24\,m}_{unknown}$ and **(c)** $P^{1\,m}_{unknown}$ are plotted against the photolytic loss rate of HONO at 24 m and 1 m above ground, respectively. The York linear fit (York et al., 2004) of $P^{24\,m}_{unknown}$ with $L^{24\,m}_{phot}$ and $P^{1\,m}_{unknown}$ with $L^{1\,m}_{phot}$ yields in $P^{24\,m}_{unknown} = -(0.93 \pm 0.05) \times L^{24\,m}_{phot} + (0.9 \pm 14.2) \times 10^3$ molecules cm^{-3} s^{-1} and $P^{1\,m}_{unknown} = -(0.96 \pm 0.08) \times L^{1\,m}_{phot} + (0.6 \pm 11.9) \times 10^3$ molecules cm^{-3} s^{-1}, respectively.